Marine heat waves’ impact on zooplankton populations and implications for biogeochemical cycling

Yoav Pinto
12/13/2022
Yoav.pinto1@gmail.com

Abstract

Climate change is causing marine heat waves to become more common, leading to increased stratification of the water column. This in turn causes hypoxic events and reduced mixing between the surface layer and the deep ocean. Food webs rely on nutrients brought up by this mixing, and marine heat waves can disrupt this process, impacting zooplankton populations through bottom-up interactions with their main food source, phytoplankton. In the Salish Sea, this nutrient rich water comes from the North Pacific through the Strait of Juan de Fuca and up into the San Juan Channel. Zooplankton populations from 2007 – 2022 were examined in the channel during the fall to determine whether a marine heat wave known as The Blob affected zooplankton diversity and abundance. The Blob formed in the North Pacific in 2013 and lasted until 2016. It was followed by several years of abnormally high sea surface temperatures (SST) lasting until the present day (2022). Years before The Blob reached the Salish Sea (2007 – 2013) were compared with years after it arrived (2014 – 2022). After the heat wave, zooplankton densities were lower at the Pelagic Ecosystem Functions’ North ($p = 0.0079$) and South ($p = 0.0026$) stations while diversity was unchanged ($p > 0.05$ at both stations). This was driven mainly by patterns in copepod dominance. Zooplankton are vital to commercially important fisheries in the Salish Sea, as well as for biogeochemical cycling. Future marine heat waves could continue to affect zooplankton populations, potentially destabilizing the ecosystem in the Salish Sea.

Introduction

Anthropogenic climate change has already made significant changes to the natural environment around the world (IPCC 2022). As the human population grows, the activities that contribute to climate change will continue to grow assuming a business-as-usual scenario. In the 2022 IPCC report, Working Group 1 (WGI) found that in the years 2011-2020, global surface temperatures have increased by 0.95 to 1.20°C above 1850–1900 temperatures. When considering all five assessed scenarios, ranging from very low greenhouse gas emissions to very high greenhouse gas emissions, WGI estimated that there is a greater than 50% chance of global temperature increase to exceed 1.5°C by 2040. As the Earth continues to warm, so too do the oceans (Levitus et al, 2012). Marine heat waves (MHW) have become more common and more widespread. The area of the ocean experiencing strong (category II) heat waves has increased by 24% from 1983 to 2018 (Hobday et al, 2018). When the surface ocean is warmed by the sun, the mixed layer becomes shallower and exchange between the surface and deep ocean slows. This can lead to hypoxia because warmer water can hold less dissolved gas than cold water and increased stratification prevents dissolved oxygen from reaching below the mixed layer (Keeling et al, 2010). These effects are further compounded by biological processes such as eutrophication (Carpenter, 2005; Stow et al, 2005) and increased levels of respiration, both in prokaryotes (Smith et al, 2019) and eukaryotes (Harris et al, 2006). As of 2008, the number of reported hypoxic locations had increased exponentially at a rate of 5.54% year over year since the early 1900s (Vaquer-Sunyer & Duarte, 2008). These changes are concerning in part because low oxygen levels can directly cause large-scale mortality events in various taxa (Vaquer-Sunyer & Duarte, 2008), which can have cascading effects throughout the food web. Changes in mixed layer dynamics can also affect the timing of phytoplankton blooms, causing average annual biomass to shift away from dominant species such as diatoms (Chiba et al, 2012; Hinder et al, 2012). This exerts a bottom-up pressure on higher trophic levels, and may disrupt nutrient cycling.

The Salish Sea, where this time series was conducted, is a large estuary on the Northwestern coast of North America. It comprises the Strait of Georgia to the North, the Strait of Juan de Fuca to the West, and the Puget Sound to the South. The Strait of Juan de Fuca is the main source of Pacific Ocean water to the Salish Sea. Tidal inflow averaged approximately 143 × 103 m^3 s^{-1} in 2014, roughly 10-20 times larger than river inflow (Khangaonkar et al, 2019). As such, the Salish Sea is mainly sensitive to changes in the properties of Pacific Ocean water. This is relevant due to elevated sea surface temperatures in the North Pacific during the North Pacific Marine Heat Wave (“The Blob”) which started forming in 2013, peaked in 2015, and after which SST remained elevated until 2021 (Barkhordarian et al, 2022). Sea surface temperatures are still above normal as of the time of this writing. Our study site is in the San Juan Archipelago, a group of islands located between the Strait of Georgia and Strait of Juan de Fuca. The San Juan Channel runs through the center of the archipelago and is characterized by strong tidal inflow from the Strait of Juan de Fuca to the South which brings in Pacific Ocean water.

This study focuses on the effects of MHWs on zooplankton in the San Juan Channel. Zooplankton are a good indicator of changes in the marine environment - they are ubiquitous, abundant, and sensitive to environmental changes (Keister et al, 2022). They are also an important link in the marine food web, serving as the primary grazers of phytoplankton in the ocean (Strom et al, 2007; Richardson, 2008) and are preyed upon by animals spanning multiple orders of magnitude, up to and including the largest organisms on earth, baleen whales (Richardson, 2008). In the Salish Sea, they are a major food source for forage fish, particularly the Pacific Sand Lance, *Ammodytes personatus* which feed primarily on zooplankton and are a known food source for 97 species in the Salish Sea including commercially important and endangered species (Sisson & Baker, 2017). Zooplankton are also an integral part of nutrient cycling. Zooplankton respiration accounts for large amounts of dissolved inorganic carbon (DIC) recycling (Hernández-León & Ikeda, 2005; Darnis & Fortier, 2012; Mayzaud & Pakhomov, 2014; McKinnon et al, 2015), and their vertical migration may at times be responsible for greater carbon export to deep water than is gravity (Darnis & Fortier, 2012). Their sloppy feeding habits, excretions, and fecal pellets return dissolved and particulate organic carbon (Møller et al, 2003; Alcaraz et al, 2010), nitrogen (Alcaraz et al, 2010; Ikeda, 2014) and phosphorous (Alcaraz et al, 2010) to the water.

Methods

Study site and sampling dates

All samples were collected from the University of Washington’s Friday Harbor Labs North (48.583ºN, 123.043ºW) and South (48.420ºN, 122.943ºW) stations (Fig. 1) aboard the R/V Centennial, R/V Kittiwake, and R/V Rachel Carson. The years included in this study are 2007 – 2022 excluding 2017 and 2020 for which data was not available. Cruise dates varied each year, but all fell within the period between late September and mid-November. Five to eight cruises were undertaken each year, with variability due to weather conditions or scheduling.

Zooplankton sampling and analysis

Zooplankton were collected by deploying a net with a 0.7 m diameter opening, and a 153 µm mesh size cod end into the water to approximately 5 - 10 m above the seafloor which is at a depth of approximately 120 m at North station and 80 m at South station before being raised to the surface. From 2018 onwards, the net was equipped with a TSK flowmeter calibrated to the diameter of the net opening; this allows the user to simply multiply the flowmeter reading by a factor matched to the net opening diameter and thus determine the total volume of water filtered. After being returned to the deck, nets were washed from the inside out using a seawater hose to collect the sample in the cod end, and samples were placed in jars with varying amounts and concentrations of borax-buffered formalin. One to three tow replicates were taken at each station. When more than one tow was conducted, I report the average zooplankton density.

The volume of water filtered was calculated by either multiplying the length of cable paid out (*l*) by the area of the net opening:

$$V = \pi r^2 \times l$$

Or by multiplying the flowmeter reading by 0.755:

$$Volume\ Filtered\ (m^3) = Flow\ ct * 0.0755$$

In the lab, the formalin was rinsed off the samples by pouring them through either a sieve or several sieves of varying mesh sizes. In all cases, the final mesh size was no larger than 118 µm. Large organisms were removed and counted individually on a lightbox. Aliquots were either taken directly from the remaining sample using a Stempel pipette, or the sample was split using a Folsom splitter until a desired density of individuals was reached, at which point they were diluted to a known volume and an aliquot was taken. Aliquots were placed in a Bogorov tray and counted using a dissecting microscope. Counts were replicated between 1 and 3 times for each sampling event, depending on the year.

When large taxa were not removed before subsampling, zooplankton density was calculated using the following formula:

$$D = \frac{N * S}{V(f * a)}$$

where D = density (individuals m^{-3}), N = the count of all organisms in subsample, S = the split volume in mL, f = the split dilution fraction, a = the aliquot volume in mL, and V = the total tow volume of water in filtered (m^{-3}).

When large taxa were removed before subsampling, the number of individuals in a sample was calculated using the following formula:

$$Ind = W + \left(\frac{S * Vd}{Vs * f}\right)$$

where *Ind* = individuals, *W* = the total number of large organisms removed, *S* = total individuals in the subsample, *Vd* = total diluted volume of the split, *Vs* = volume of subsample used for counting, and *f* = fraction of the whole sample that was counted. This number was then divided by the total volume filtered during the tow to return density.

Marine heat wave severity determination

Marine heat wave severity was ranked on a 0 – IV scale, with 0 as normal conditions and IV as an extreme heat wave. Data was taken from the Marine Heatwave Tracker, http://www.marineheatwaves.org/tracker.html. Scores were given based on conditions in the Pacific Ocean in the vicinity of the entrance to the Strait of Juan de Fuca and cross-referenced with Suryan et al, 2021.

Data analysis

Datasheets were compiled and taxa were organized to the lowest possible category without causing categories to overlap or to be excluded. Data was analyzed using R version 4.2.2. Density was calculated for the total sample and copepods & their nauplii. Two diversity indices were taken for each sampling date and each station. The Shannon-Wiener diversity index describes the uncertainty in the taxonomic identity of an unknown individual (Morris et al, 2014):

$$H' = -\Sigma P_i \ln{(P_i)}$$

and the inverse Simpson's index for dominance. The original Simpson's index is a representation of the probability that two randomly chosen individuals belong to the same group. However, this gives lower values for higher diversity, which is counterintuitive. Therefore, the inverse is used, in which case higher values mean a higher diversity (Morris et al, 2014). It is an indirect representation of the probability that two randomly selected individuals belong to different groups. The formula is given by:

$$D_2 = 1/\Sigma^{P_i^2}$$

Where in both equations P_i is the proportion of species belonging to species *i*.

Total density and copepod density as well as diversity indices were plotted for each year and compared across MHW and non-MHW years. Additionally, relative densities were plotted for each year.

ANOVA

Years pre- and post-MHW were grouped in two ways. First, the years were split into groupings before and after The Blob (2007 – 2012, 2013 – 2022). Second, the years were split into groupings before The Blob and including its first year (2007 – 2013) and the years after that (2014 – 2022). This was done to determine if the effects of the first year of the MHW were significant. One-way ANOVA tests were done on total densities and the diversity indices before and after The Blob (2007 – 2012 vs 2013 – 2022 and 2007 – 2013 vs 2014 – 2022).

Results

Offset group (2007 – 2013 vs 2014 – 2022)

Zooplankton density was greater in years before the MHW and its first year (North mean ≈ 4135 ind m^{-3} 217; South mean ≈ 5837 ind m^{-3} 397) than in the second year of the MHW to the present (North mean ≈ 2356 ind m^{-3}, ± 515; South mean ≈ 2966 ind m^{-3}, ± 640). The ANOVA comparing pre- and during-MHW densities returned significant results (North $p \approx 0.0079$, South $p \approx 0.0025$). In the offset pre-MHW years, the average inverse Simpson's index was 1.93 ± 0.253 at North station and 1.67 ± 0.221 at South Station. The Shannon indices for the same years were 0.953 ± 0.148 at North and 0.780 ± 0.154 at South. After the MHW, the Simpson's indices were 1.82 ± 0.163 at North and 1.60 ± 0.113 at South. The Shannon indices were 0.925 ± 0.119 at North and 0.758 ± 0.108 at South. These results are summarized in table 1.

Non-offset group (2007 – 2012 vs 2013 – 2022)

The difference was smaller when comparing exclusively pre-MHW years, 2007 – 2012 (North mean ≈ 4041 ind m^{-3} ± 232; South mean ≈ 5636 ind m^{-3} ± 405) with post-MHW years, 2013 – 2022 (North mean ≈ 2649 ind m^{-3} ± 534; South mean ≈ 3475 ind m^{-3} ± 753) and the ANOVA results were not significant at North ($p \approx 0.172$) and significant at South ($p \approx 0.0027$). In the non-offset grouping, pre-MHW (2007 – 2012) Simpson indices were 1.94 ± 0.299 at North and 1.74 ± 0.248 at South, while Shannon's indices were 0.973 ± 0.173 at North and 0.832 ± 0.172 at South. In post-MHW years (2013 – 2022) the Simpson's indices were 1.83 ± 0.142 at North and 1.55 ± 0.111 at South. Shannon's indices were 0.914 ± 0.104 at North and 0.722 ± 0.100 at South. These results are summarized in table 2.

Summary

Diversity did not differ significantly when compared across MHW and non-MHW years, neither in the offset nor in the non-offset groupings. Density differences between years were greater at South Station than at North Station in both the offset and non-offset grouping. The density difference in the offset grouping was greater than in the non-offset grouping.

Copepods & their nauplii

Copepod density was higher in 2007 – 2013 than in 2014 – 2022 for both North and South stations, while nauplii density did not differ significantly. The average copepod density at North station from 2007 – 2013 was ≈ 2298 ind m^{-3} ± 250 and from 2014 – 2022 it was ≈ 1391 ind m^{-3} ± 238 ($p \approx 0.0222$). In the same years, nauplii density was ≈ 928 ± 218 and ≈ 746 ± 266 respectively ($p \approx 0.53$). At South Station, copepod density from 2007 – 2013 was ≈ 3577 ind m^{-3} ± 458 and nauplii density was ≈ 928 ind m^{-3} ± 182. In 2014 – 2022, copepod density was ≈ 1846 ind m^{-3} ± 354 ($p \approx 0.0113$) and nauplii density was ≈ 484 ind m^{-3} ± 148 ($p \approx 0.179$). These results are summarized in table 3.

Discussion

In heat wave years, the bulk of the anomalous temperatures were in the Northern Pacific Ocean rather than in the Salish Sea itself. This water enters the Salish Sea through the Strait of Juan de Fuca due to tidal forces but fails to leave the same way due to the sills present throughout the estuary trapping dense, saltier ocean water. While warmer water is typically less dense than colder water, freshwater influx from the various rivers draining into the Salish Sea forms the main bulk of water leaving the Sea, causing the abnormally warm but still salty water from the Pacific Ocean to remain trapped in the estuary. The sheltered nature of the San Juan Channel and the sill present at Cattle Pass may prevent part of the warm water mass from reaching the North station, while the South station is more exposed to oceanic conditions. This may explain why populations at the Southern station decreased more in post-MHW years relative to the North station (Tables 1 and 2; figures 2 – 6). The presence of abnormally warm water decreases mixing between the surface layer and the deep layer (Keeling et al, 2010), which may be the root of the changes seen during MHW years.

Zooplankton populations are impacted by MHW events, with populations at both North and South stations being significantly lower when comparing the years pre-MHW and including the first year of the MHW to years post-MHW (Figures 2 – 6). This could indicate one of two things. First, there may be a delay in the effects of oceanic heating on zooplankton populations. Second, in 2013, the year The Blob began to take shape, the magnitude of the heating was relatively moderate compared to later years. This may not have been enough to cross the threshold at which zooplankton populations begin to react. Zooplankton generally have a life cycle shorter than one year, suggesting that the reason for the delay in zooplankton population reaction was that a certain threshold was not crossed until sometime after the 2013 PEF session. Previous studies have shown that interannual climate variations impact zooplankton (Molinero et al, 2018), potentially through bottom-up interactions with phytoplankton which show changes in both community composition in response to interannual climate variations (Chiba et al, 2012; Hinder et al, 2012) and phenology in response to seasonal temperature differences (Chiba et al, 2012). In particular, Chiba et al found that changes in phytoplankton spring bloom timing could shift biomass away from diatoms. This was likely driven by mixed layer dynamics & how they influence nutrients and light availability for phytoplankton.

Interannual diversity was not affected by The Blob. Intra-annually, the Shannon’s and Simpson’s diversity indices generally followed the same pattern (Figures 7 – 11), indicating that when diversity was higher, it was due to the dominant taxon densities being lower, which in this study were copepods. When copepod dominance was lower, it was generally the result of larger numbers of tunicates (Figures 17 – 21). There were two years during which this pattern was broken. In 2008 there was a dinoflagellate bloom early in the season (Figure 17) which was followed by lower zooplankton densities (Figure 2). In 2016 the density of crustacean larvae was abnormally high, as was the total zooplankton density. However, increasing numbers of adult copepods were not seen in the following weeks, suggesting that there were large numbers of non-copepod larvae in the water. Overall diversity trends may be driven by the success of copepods, although the driving force behind this remains unclear and should be further examined. In warmer waters, zooplankton communities are characterized by smaller members of similar taxa than in colder waters (Stempniewicz et al, 2007), which the PEF density data would not capture. Further investigation during future MHWs should examine the size composition of zooplankton populations. If this is the case in the Salish Sea then prolonged marine heat waves may result in zooplankton populations that are both less dense and comprise smaller individuals. The two effects may synergize and impact higher trophic levels more than either effect alone which may impact commercial fisheries. Copepods comprise a large part of the diet for juvenile salmon (Armstrong et al, 2008) and shifts in their population are correlated to juvenile salmon survival (Keister et al, 2022) which implies that if zooplankton communities are disrupted by future MHWs, those fisheries may be disrupted as well.

Marine heat waves may also disrupt the complex network of processes that drive biogeochemical cycling in the Salish Sea. Zooplankton populations may remain low when MHWs happen repeatedly over the course of relatively short periods, as has been seen in the Salish Sea in the years since The Blob. With that decrease comes a decrease in total respiration done in the water column and smaller amounts of nutrients being released through their excretions, fecal pellets, and sloppy feeding. Of special importance is nitrogen. In the Salish Sea, phytoplankton populations are dominated by diatoms which form the bulk of annual phytoplankton biomass (Del Bel Belluz et al, 2021) and whose growth tends to be nitrogen limited (Khangaonkar et al, 2018). When zooplankton populations decrease, this return of nutrients slows and may limit diatom growth, which creates a positive feedback loop in which zooplankton which graze on diatoms have less food available. This potential feedback loop suggests that decreasing zooplankton populations in response to MHW and oceanic heating in general may drive decreasing carbon export to the deep ocean, thereby exacerbating climate change.

Citations

Alcaraz, M., Almeda, R., Calbet, A., Saiz, E., Duarte, C. M., Lasternas, S., Agustí, S., Santiago, R., Movilla, J., & Alonso, A. (2010). role of arctic zooplankton in biogeochemical cycles: respiration and excretion of ammonia and phosphate during summer. *Polar Biology*, *33*(12), 1719–1731. https://doi.org/10.1007/s00300-010-0789-9

Armstrong, J. L., Myers, K. W., Beauchamp, D. A., Davis, N. D., Walker, R. V., Boldt, J. L., Piccolo, J. J., Haldorson, L. J., & Moss, J. H. (2008). Interannual and Spatial Feeding Patterns of Hatchery and Wild Juvenile Pink Salmon in the Gulf of Alaska in Years of Low and High Survival, *Transactions of the American Fisheries Society (1900)*, *137*(5), 1299–1316. https://doi.org/10.1577/T07-196.1

Barkhordarian, A., Nielsen, D. M., & Baehr, J. (2022). Recent marine heatwaves in the North Pacific warming pool can be attributed to rising atmospheric levels of greenhouse gases. *Communications Earth & Environment*, *3*(1), 1–12. https://doi.org/10.1038/s43247-022-00461-2

Carpenter, S. . (2005). Eutrophication of aquatic ecosystems: bistability and soil phosphorus. Proceedings of the National Academy of Sciences - PNAS, 102(29), 10002–10005. https://doi.org/10.1073/pnas.0503959102

Chiba, S., Batten, S., Sasaoka, K., Sasai, Y., & Sugisaki, H. (2012). Influence of the Pacific Decadal Oscillation on phytoplankton phenology and community structure in the western North Pacific. *Geophysical Research Letters*, *39*(15). https://doi.org/10.1029/2012GL052912

Darnis, G., & Fortier, L. (2012). Zooplankton respiration and the export of carbon at depth in the Amundsen Gulf (Arctic Ocean). *Journal of Geophysical Research: Oceans*, *117*(C4). https://doi.org/10.1029/2011JC007374

Del Bel Belluz, J., Peña, M. A., Jackson, J. M., & Nemcek, N. (2021). Phytoplankton Composition and Environmental Drivers in the Northern Strait of Georgia (Salish Sea), British Columbia, Canada. *Estuaries and Coasts*, *44*(5), 1419–1439. https://doi.org/10.1007/s12237-020-00858-2

H. Wickham. ggplot2: Elegant Graphics for Data Analysis. Springer-Verlag New York, 2016.

HARRIS, L. A., DUARTE, C. M., & NIXON, S. W. (2006). Allometric Laws and Prediction in Estuarine and Coastal Ecology. Estuaries and Coasts, 29(2), 340–344. https://doi.org/10.1007/BF02782002

Hinder, S. L., Hays, G. C., Edwards, M., Roberts, E. C., Walne, A. W., & Gravenor, M. B. (2012). Changes in marine dinoflagellate and diatom abundance under climate change. *Nature Climate Change*, *2*(4), 271–275. https://doi.org/10.1038/NCLIMATE1388

Hernández-León, S., & Ikeda, T. (2005). A global assessment of mesozooplankton respiration in the ocean. *Journal of Plankton Research*, *27*(2), 153–158. https://doi.org/10.1093/plankt/fbh166

Hobday, A., Oliver, E., Sen Gupta, A., Benthuysen, J., Burrows, M., Donat, M., Holbrook, N., Moore, P., Thomsen, M., Wernberg, T., & Smale, D. (2018). Categorizing and Naming MARINE HEATWAVES. *Oceanography (Washington, D.C.)*, *31*(2), 162–173. https://doi.org/10.5670/oceanog.2018.205

Ikeda, T. (2014). Respiration and ammonia excretion by marine metazooplankton taxa: synthesis toward a global-bathymetric model. *Marine Biology*, *161*(12), 2753–2766. https://doi.org/10.1007/s00227-014-2540-5

https://tidesandcurrents.noaa.gov/waterlevels.html?id=9449880

Kassambara A (2022). _ggpubr: 'ggplot2' Based Publication Ready Plots_. R package version 0.5.0, https://CRAN.R-project.org/package=ggpubr

Keeling, R. F., Koertzinger, A., & Gruber, N. (2010). Ocean Deoxygenation in a Warming World. Annual Review of Marine Science, 2(1), 199–229. https://doi.org/10.1146/annurev.marine.010908.163855

Keister, J. E., Herrmann, B., & Bos, J. (2022). Zooplankton composition links to climate and salmon survival in a northern temperate fjord. Limnology and Oceanography, 67(11), 2389–2404. https://doi.org/10.1002/lno.12208

Khangaonkar, T., Nugraha, A., Xu, W., Long, W., Bianucci, L., Ahmed, A., Mohamedali, T., & Pelletier, G. (2018). Analysis of Hypoxia and Sensitivity to Nutrient Pollution in Salish Sea. *Journal of Geophysical Research. Oceans*, *123*(7), 4735–4761. https://doi.org/10.1029/2017JC013650

Khangaonkar, T., Nugraha, A., Xu, W., & Balaguru, K. (2019). Salish Sea Response to Global Climate Change, Sea Level Rise, and Future Nutrient Loads. Journal of Geophysical Research. Oceans, 124(6), 3876–3904. https://doi.org/10.1029/2018JC014670

Lemon, J. (2006) Plotrix: a package in the red light district of R. R-News, 6(4): 8-12

Levitus, S., Antonov, J. I., Boyer, T. P., Baranova, O. K., Garcia, H. E., Locarnini, R. A., Mishonov, A. V., Reagan, J. R., Seidov, D., Yarosh, E. S., & Zweng, M. M. (2012). World ocean heat content and thermosteric sea level change (0-2000 m), 1955-2010. *Geophysical Research Letters*, *39*(10). https://doi.org/10.1029/2012GL051106

Marc J. Mazerolle (2020) AICcmodavg: Model selection and multimodel inference based on (Q)AIC(c). R package version 2.3-1. https://cran.r-project.org/package=AICcmodavg

MAYZAUD, P., & PAKHOMOV, E. A. (2014). The role of zooplankton communities in carbon recycling in the Ocean: the case of the Southern Ocean. *Journal of Plankton Research*, *36*(6), 1543–1556. https://doi.org/10.1093/plankt/fbu076

McKinnon, A. D., Doyle, J., Duggan, S., Logan, M., Lønborg, C., & Brinkman, R. (2015). Zooplankton Growth, Respiration and Grazing on the Australian Margins of the Tropical Indian and Pacific Oceans. *PloS One*, *10*(10), e0140012–e0140012. https://doi.org/10.1371/journal,pone.0140012

Molinero, J. C., Tseng, L.-C., Lopez Abbate, C., Ramirez-Romero, E., & Hwang, J.-S. (2018). Interannual changes in zooplankton echo subtropical and high latitude climate effects in the southern East China Sea. *PloS One*, *13*(5), e0197382–e0197382. https://doi.org/10.1371/journal,pone.0197382

MØLLER, E. F., THOR, P., & NIELSEN, T. G. (2003). Production of DOC by Calanus finmarchicus, C. glacialis and C. hyperboreus through sloppy feeding and leakage from fecal pellets. *Marine Ecology. Progress Series (Halstenbek)*, *262*, 185–191. https://doi.org/10.3354/meps262185

Morris, E. K., Caruso, T., Buscot, F., Fischer, M., Hancock, C., Maier, T. S., Meiners, T., Müller, C., Obermaier, E., Prati, D., Socher, S. A., Sonnemann, I., Wäschke, N., Wubet, T., Wurst, S., & Rillig, M. C. (2014). Choosing and using diversity indices: insights for ecological applications from the German Biodiversity Exploratories. *Ecology and Evolution*, *4*(18), 3514–3524. https://doi.org/10.1002/ece3.1155

Oksanen J, Simpson G, Blanchet F, Kindt R, Legendre P, Minchin P, O'Hara R, Solymos P, Stevens M, Szoecs E, Wagner H, Barbour M, Bedward M, Bolker B, Borcard D, Carvalho G, Chirico M, De Caceres M, Durand S, Evangelista H, FitzJohn R, Friendly M, Furneaux B, Hannigan G, Hill M, Lahti L, McGlinn D, Ouellette M, Ribeiro Cunha E, Smith T, Stier A, Ter Braak C, Weedon J (2022). _vegan: Community Ecology Package_. R package version 2.6-4, <https://CRAN.R-project.org/package=vegan>.

Pörtner, H.-O., D.C. Roberts, H. Adams, I. Adelekan, C. Adler, R. Adrian, P. Aldunce, E. Ali, R. Ara Begum, B. Bednar- Friedl, R. Bezner Kerr, R. Biesbroek, J. Birkmann, K. Bowen, M.A. Caretta, J. Carnicer, E. Castellanos, T.S. Cheong, W. Chow, G. Cissé, S. Clayton, A. Constable, S.R. Cooley, M.J. Costello, M. Craig, W. Cramer, R. Dawson, D. Dodman, J. Efitre, M. Garschagen, E.A. Gilmore, B.C. Glavovic, D. Gutzler, M. Haasnoot, S. Harper, T. Hasegawa, B. Hayward, J.A. Hicke, Y. Hirabayashi, C. Huang, K. Kalaba, W. Kiessling, A. Kitoh, R. Lasco, J. Lawrence, M.F. Lemos, R. Lempert, C. Lennard, D. Ley, T. Lissner, Q. Liu, E. Liwenga, S. Lluch-Cota, S. Löschke, S. Lucatello, Y. Luo, B. Mackey, K. Mintenbeck, A. Mirzabaev, V. Möller, M. Moncassim Vale, M.D. Morecroft, L. Mortsch, A. Mukherji, T. Mustonen, M. Mycoo, J. Nalau, M. New, A. Okem, J.P. Ometto, B. O'Neill, R. Pandey, C. Parmesan, M. Pelling, P.F. Pinho, J. Pinnegar, E.S. Poloczanska, A. Prakash, B. Preston, M.-F. Racault, D. Reckien, A. Revi, S.K. Rose, E.L.F. Schipper, D.N. Schmidt, D. Schoeman, R. Shaw, N.P. Simpson, C. Singh, W. Solecki, L. Stringer, E. Totin, C.H. Trisos, Y. Trisurat, M. van Aalst, D. Viner, M. Wairiu, R. Warren, P. Wester, D. Wrathall, and Z. Zaiton Ibrahim, 2022: Technical Summary. [H.-O. Pörtner, D.C. Roberts, E.S. Poloczanska, K. Mintenbeck, M. Tignor, A. Alegría, M. Craig, S. Langsdorf, S. Löschke, V. Möller, A. Okem (eds.)]. In: Climate Change 2022: Impacts, Adaptation and Vulnerability. Contribution of Working Group II to the Sixth Assessment Report of the Intergovernmental Panel on Climate Change [H.-O. Pörtner, D.C. Roberts, M. Tignor, E.S. Poloczanska, K. Mintenbeck, A. Alegría, M. Craig, S. Langsdorf, S. Löschke, V. Möller, A. Okem, B. Rama (eds.)]. Cambridge University Press, Cambridge, UK and New York, NY, USA, pp. 37–118, doi:10.1017/9781009325844.002.

R Core Team (2022). R: A language and environment for statistical computing. R Foundation for Statistical Computing, Vienna, Austria. URL https://www.R-project.org/.

Richardson, A. J. (2008). In hot water: zooplankton and climate change. *ICES Journal of Marine Science*, *65*(3), 279–295. https://doi.org/10.1093/icesjms/fsn028

Robinson D, Hayes A, Couch S (2022). _broom: Convert Statistical Objects into Tidy Tibbles_. R package version 1.0.1, https://CRAN.R-project.org/package=broom

Roman, M. R., Pierson, J. J., Kimmel, D. G., Boicourt, W. C., & Zhang, X. (2012). Impacts of Hypoxia on Zooplankton Spatial Distributions in the Northern Gulf of Mexico. Estuaries and Coasts, 35(5), 1261–1269. https://doi.org/10.1007/s12237-012-9531-x

Sisson, N. B., & Baker, M. R. (2017). Feeding Ecology of Pacific Sand Lance in the San Juan Archipelago. Marine and Coastal Fisheries, 9(1), 612–625. https://doi.org/10.1080/19425120.2017.1370043

Smith, T. P., Thomas, T. J. H., García-Carreras, B., Sal, S., Yvon-Durocher, G., Bell, T., & Pawar, S. (2019). Community-level respiration of prokaryotic microbes may rise with global warming. Nature Communications, 10(1), 5124–11. https://doi.org/10.1038/s41467-019-13109-1

Stempniewicz, L., Błachowiak-Samołyk, K., & Węsławski, J. M. (2007). Impact of climate change on zooplankton communities, seabird populations and arctic terrestrial ecosystem—A scenario. *Deep-Sea Research. Part 2. Topical Studies in Oceanography*, *54*(23), 2934–2945. https://doi.org/10.1016/j.dsr2.2007.08.012

Stow, C. A., Qian, S. S., & Craig, J. K. (2005). Declining Threshold for Hypoxia in the Gulf of Mexico. Environmental Science & Technology, 39(3), 716–723. https://doi.org/10.1021/es049412o

Strom, S. L., Macri, E. L., & Olson, M. B. (2007). Microzooplankton Grazing in the Coastal Gulf of Alaska: Variations in Top-down Control of Phytoplankton. Limnology and Oceanography, 52(4), 1480–1494. https://doi.org/10.4319/lo.2007.52.4.1480

Suryan, R. M., Arimitsu, M. L., Coletti, H. A., Hopcroft, R. R., Lindeberg, M. R., Barbeaux, S. J., Batten, S. D., Burt, W. J., Bishop, M. A., Bodkin, J. L., Brenner, R., Campbell, R. W., Cushing, D. A., Danielson, S. L., Dorn, M. W., Drummond, B., Esler, D., Gelatt, T., Hanselman, D. H., … Zador, S. G. (2021). Ecosystem response persists after a prolonged marine heatwave. *Scientific Reports*, *11*(1), 6235–17. https://doi.org/10.1038/s41598-021-83818-5

Vaquer-Sunyer, R., & Duarte, C. M. (2008). Thresholds of hypoxia for marine biodiversity. Proceedings of the National Academy of Sciences - PNAS, 105(40), 15452–15457. https://doi.org/10.1073/pnas.0803833105

Wickham H, Averick M, Bryan J, Chang W, McGowan LD, François R, Grolemund G, Hayes A, Henry L, Hester J, Kuhn M, Pedersen TL, Miller E, Bache SM, Müller K, Ooms J, Robinson D, Seidel DP, Spinu V, Takahashi K, Vaughan D, Wilke C, Woo K, Yutani H (2019). “Welcome to the tidyverse.” _Journal of Open Source Software_, *4*(43), 1686. doi:10.21105/joss.01686 https://doi.org/10.21105/joss.01686

Wickham H, Bryan J (2022). _readxl: Read Excel Files_. R package version 1.4.1, <https://CRAN.R-project.org/package=readxl>.

Tables

Pre MHW (2007 - 2013)						
Station	Average Density (ind/m^3)	SE	Average Shannon's	SE	Average Simpson's	SE
North	4135	217	0.953	0.148	1.932	0.2530
South	5837	397	0.780	0.154	1.668	0.221

Post MHW (2014 - 2022)						
Station	Average Density (ind/m^3)	SE	Average Shannon's	SE	Average Simpson's	SE
North	2356** $p = 0.0079$	515	0.925 $p = 0.886$	0.119	1.820 $p = 0.715$	0.163
South	2966** $p = 0.0025$	640	0.758 $p = 0.907$	0.108	1.596 $p = 0.777$	0.118

Table 1: Summary of offset grouping statistics. Asterisks indicate levels of statistical significance between pre- and post-years within each grouping.

Pre MHW (2007 - 2012)						
Station	Average Density (ind/m^3)	SE	Average Shannon's	SE	Average Simpson's	SE
North	4041	187	0.972	0.173	1.94	0.299
South	5636	479	0.832	0.172	1.74	0.248
Post MHW (2013 - 2022)						
Station	Average Density (ind/m^3)	SE	Average Shannon's	SE	Average Simpson's	SE
North	2649 p = 0.0544	659	0.914 p = 0.764	0.104	1.83 p = 0.732	0.142
South	3475* p = 0.041	631	0.722 p = 0.569	0.1	1.55 p = 0.475	0.111

Table 1: Summary of non-offset grouping statistics. Asterisks indicate levels of statistical significance between pre- and post-years within each grouping.

Pre MHW									
2007 - 2013					2007 - 2012				
Station	Copepod Densty	SE	Nauplii Density	SE	Station	Copepod Densty	SE	Nauplii Density	SE
North	2298	250	967	218	North	2207	276	789	149
South	3577	458	928	182	South	3622	839	712	166
Post MHW									
2014 - 2022					2013 - 2022				
Station	Copepod Densty	SE	Nauplii Density	SE	Station	Copepod Densty	SE	Nauplii Density	SE
North	1391* $p = 0.0222$	238	746 $p = 0.53$	266	North	1572 $p = 0.137$	275	930 $p = 0.689$	291
South	1846* $p = 0.0113$	354	484 $p = 0.179$	148	South	2028* $p = 0.0247$	357	633 $p = 0.767$	195

Table 3: Statistics on the density of copepods and copepod nauplii. Asterisks represent the degree of statistical significance.

Figures

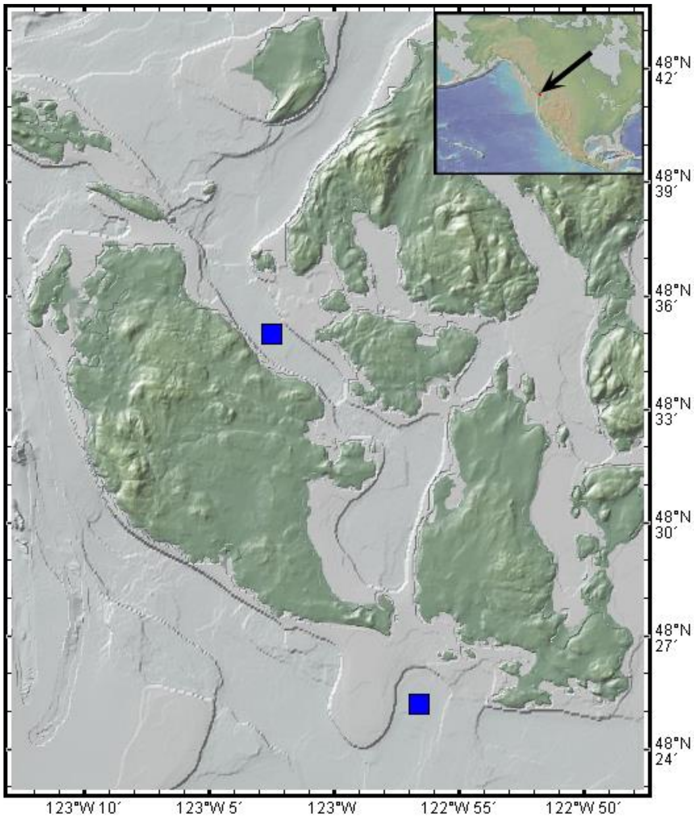

Figure 1: Map showing the north and south stations.

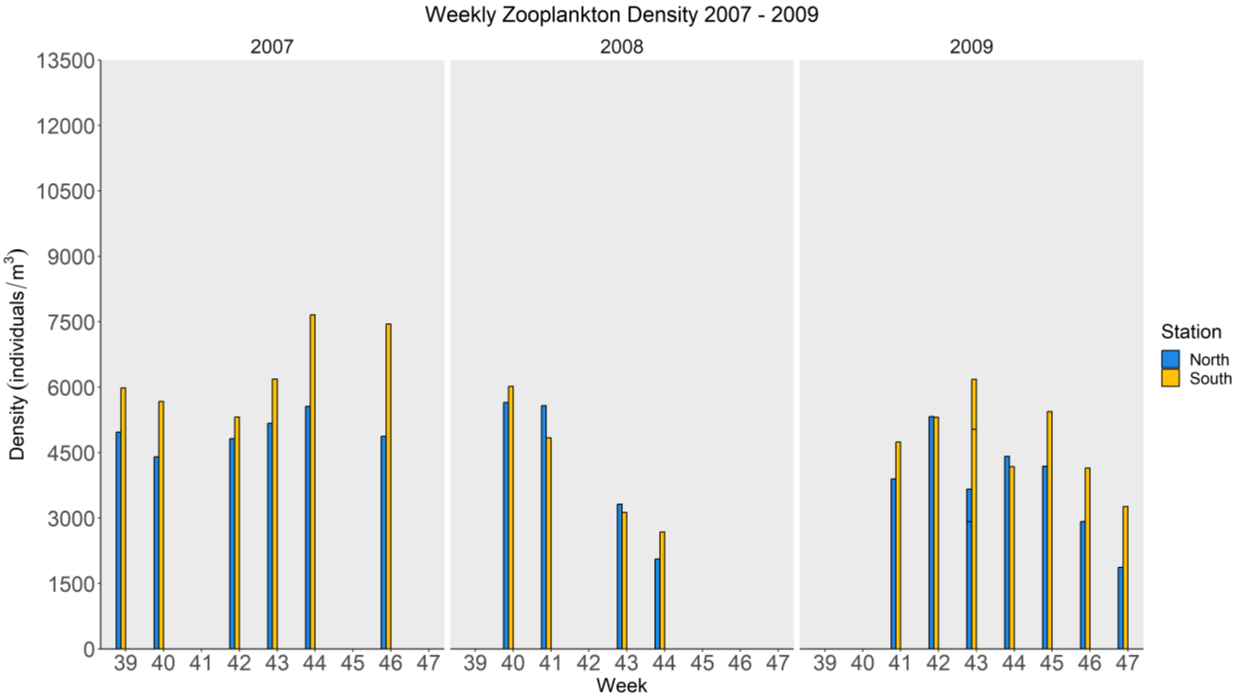

Figure 2: Weekly zooplankton density at north and south stations for 2007 – 2009.

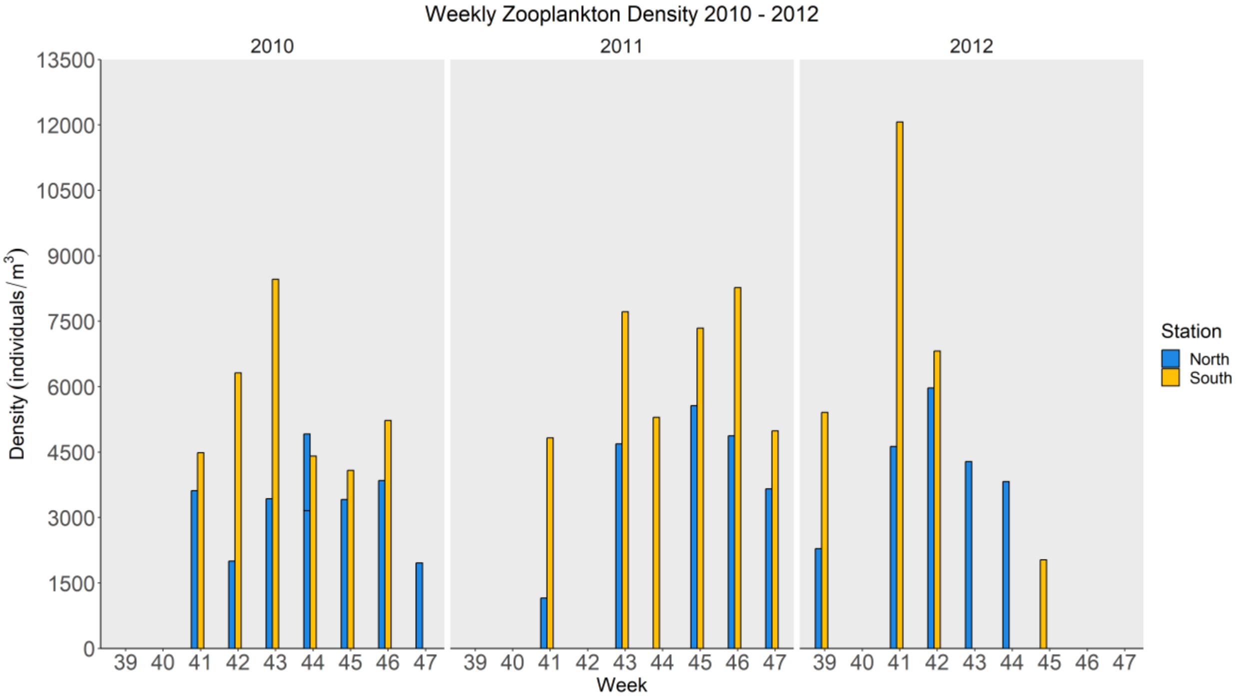

Figure 3: Weekly zooplankton density at north and south stations for 2010 – 2011.

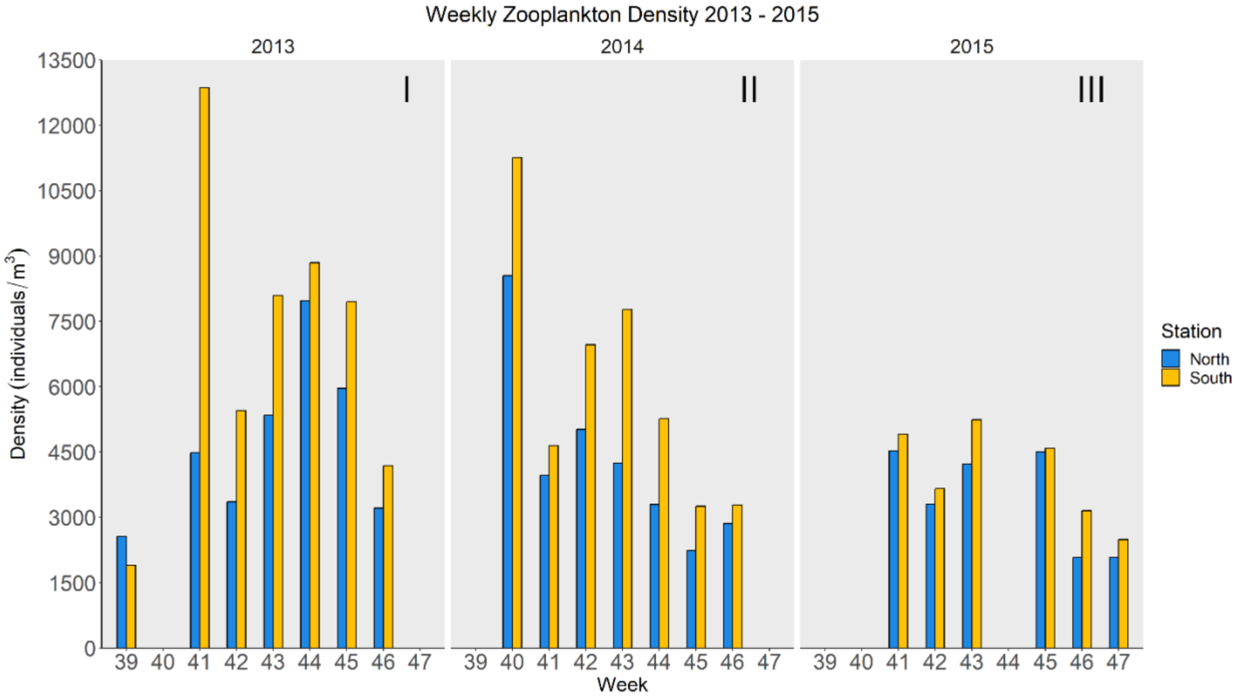

Figure 4: Weekly zooplankton density at north and south stations for 2013 – 2015. “I” indicates mild MHW conditions in the Pacific Ocean, “II” indicates moderate MHW conditions in the Pacific Ocean, and “III” indicates severe MHW conditions in the Pacific Ocean.

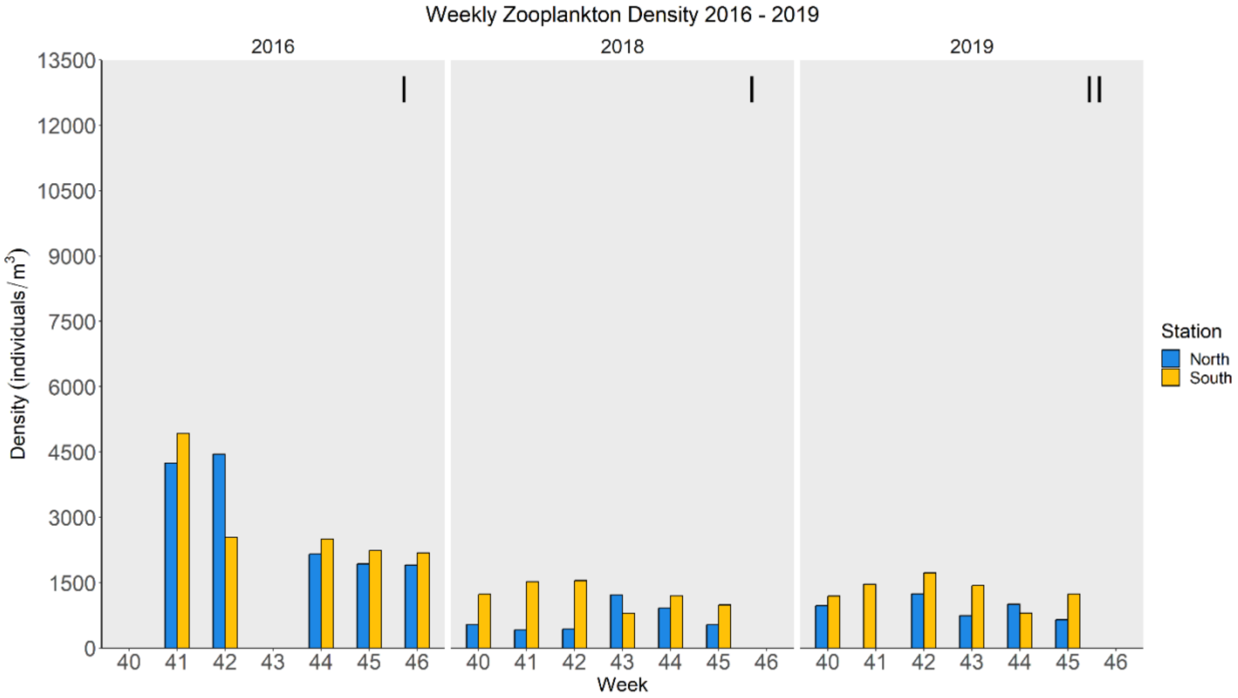

Figure 5: Weekly zooplankton density at north and south stations for 2016 – 2019. “I” indicates mild MHW conditions in the Pacific Ocean and “II” indicates moderate MHW conditions in the Pacific Ocean.

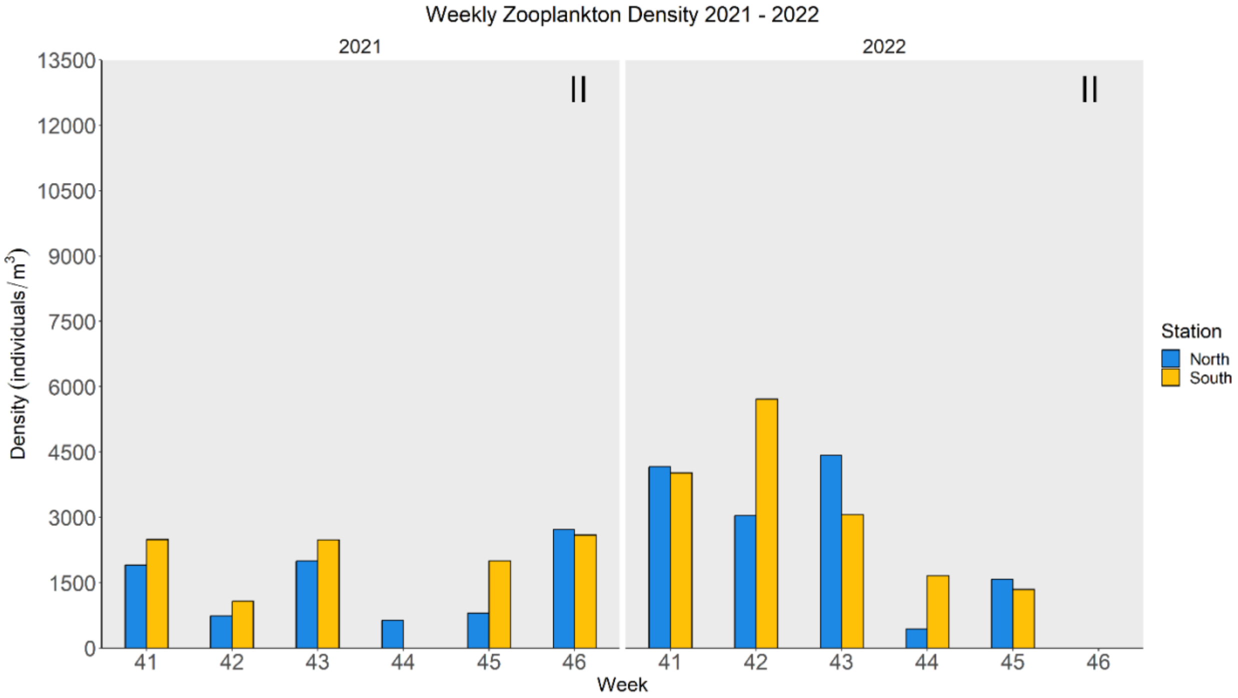

Figure 6: Weekly zooplankton density at north and south stations for 2021 and 2022. “II” indicates moderate MHW conditions in the Pacific Ocean.

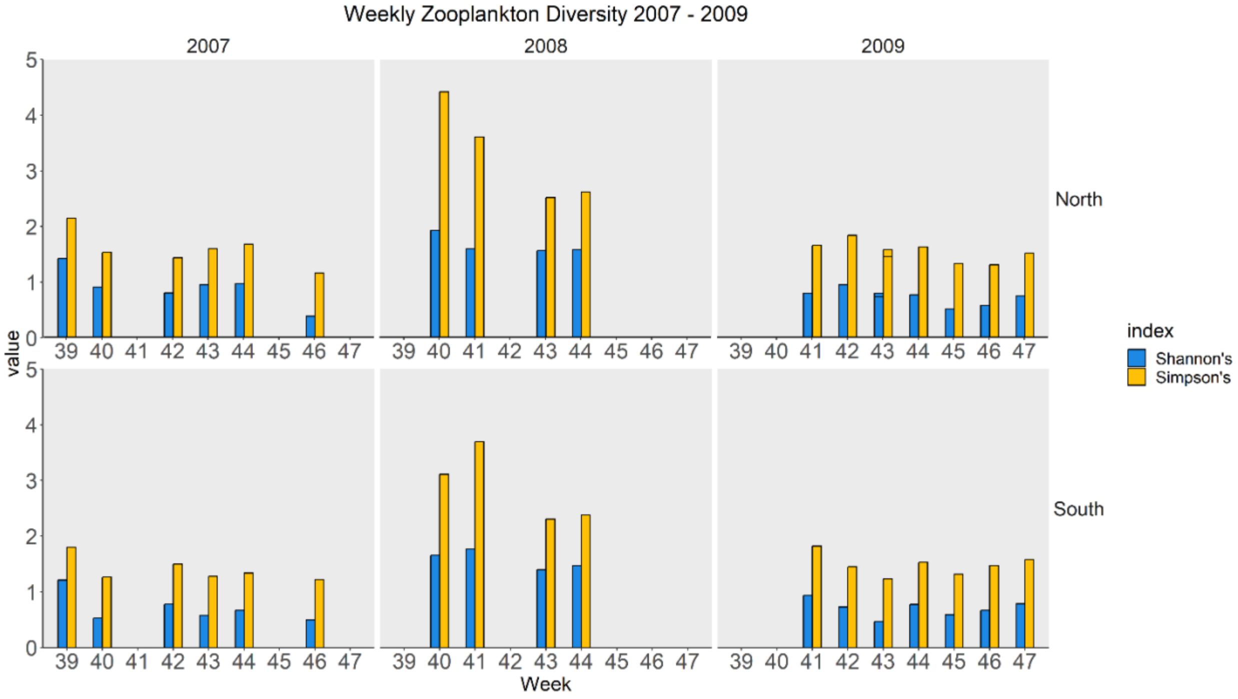

Figure 7: Weekly zooplankton diversity indices at North and South stations, 2007 – 2009.

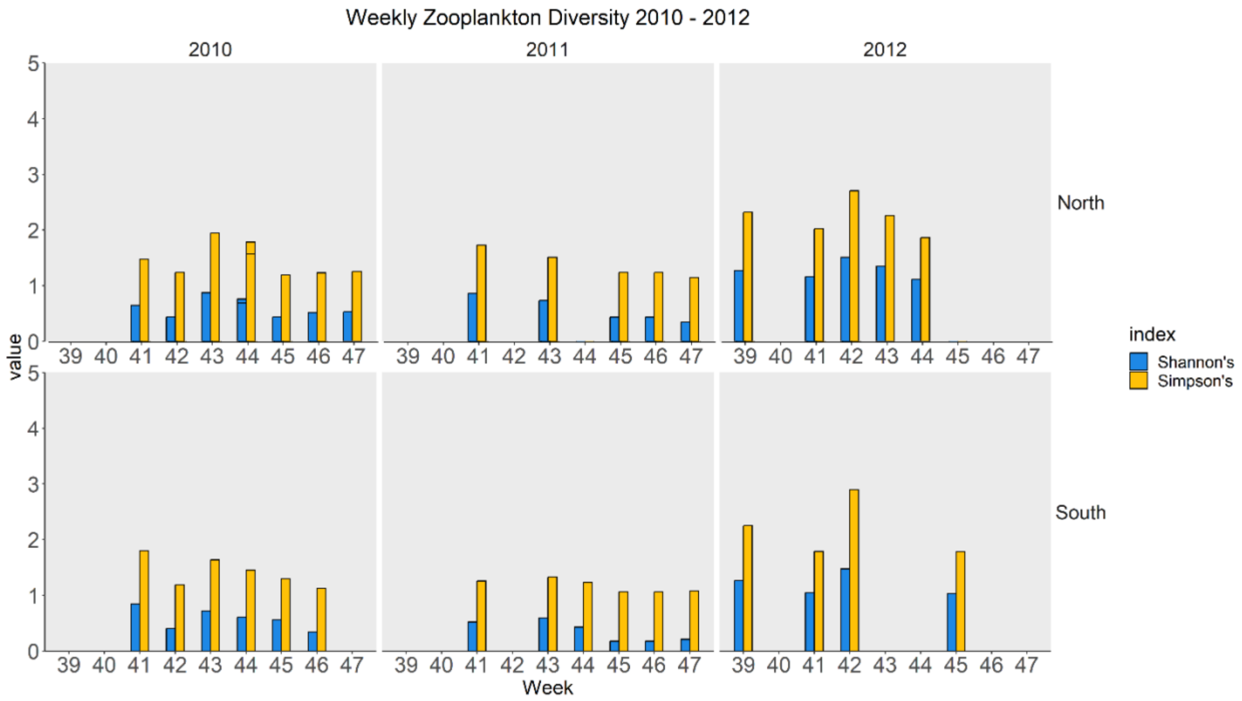

Figure 8: Weekly zooplankton diversity indices at North and South stations, 2007 – 2009.

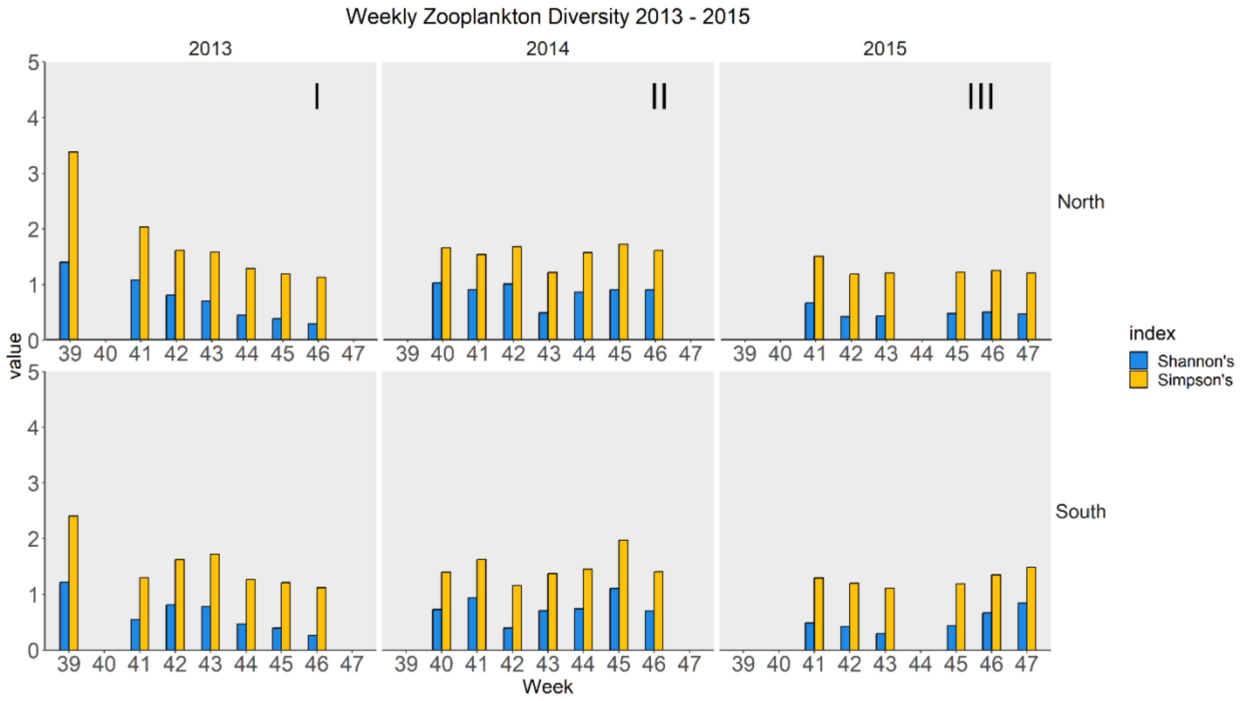

Figure 9: Weekly zooplankton diversity indices at north and south stations for 2013 – 2015. “I” indicates mild MHW conditions in the Pacific Ocean, “II” indicates moderate MHW conditions in the Pacific Ocean, and “III” indicates severe MHW conditions in the Pacific Ocean.

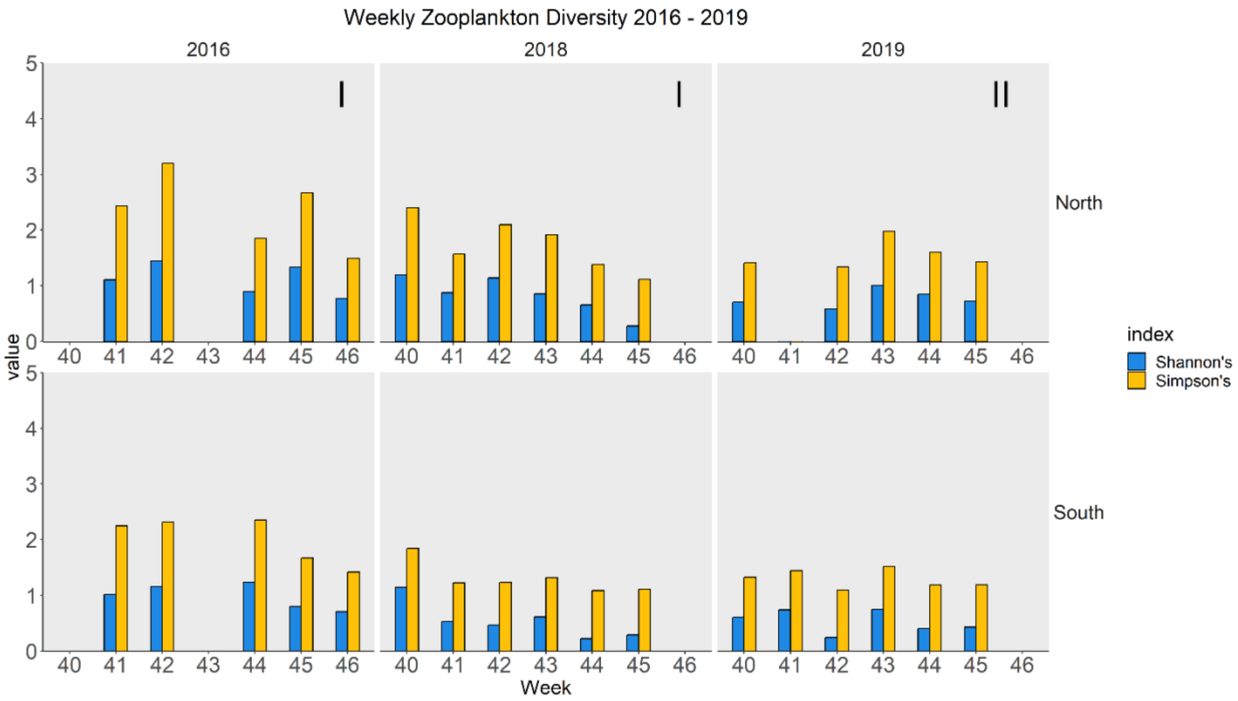

Figure 10: Weekly zooplankton diversity indices at north and south stations for 2016 – 2019. “I” indicates mild MHW conditions in the Pacific Ocean and “II” indicates moderate MHW conditions in the Pacific Ocean.

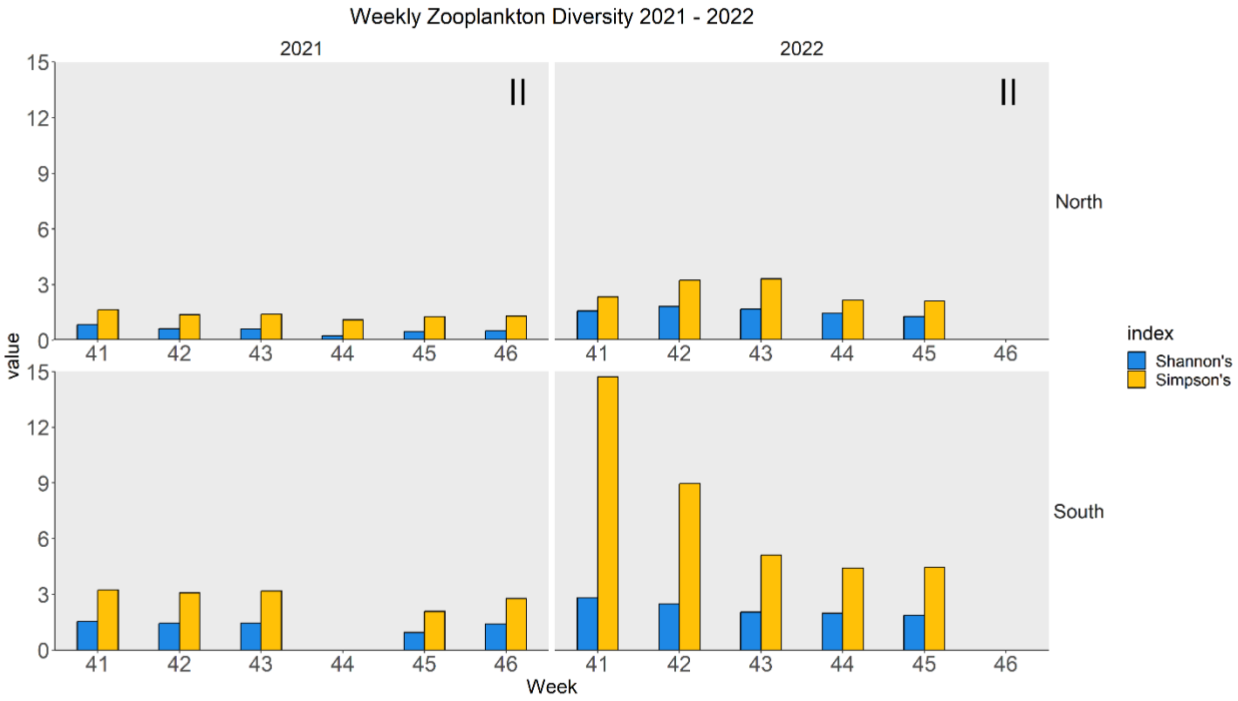

Figure 11: Weekly zooplankton diversity indices at north and south stations for 2021 and 2022. “II” indicates moderate MHW conditions in the Pacific Ocean. Note the scale has changed to accommodate high diversity on weeks 41 and 42 in 2022, South station.

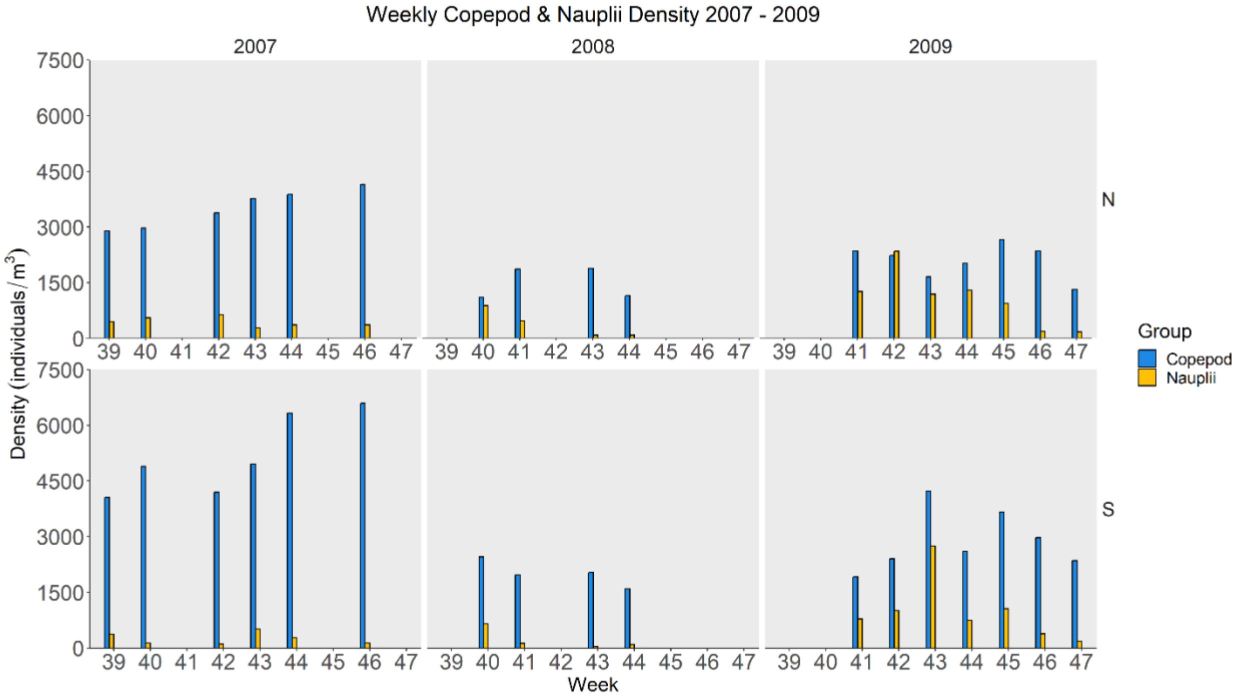

Figure 12: Weekly copepod & nauplii density at north and south stations for 2007 – 2009.

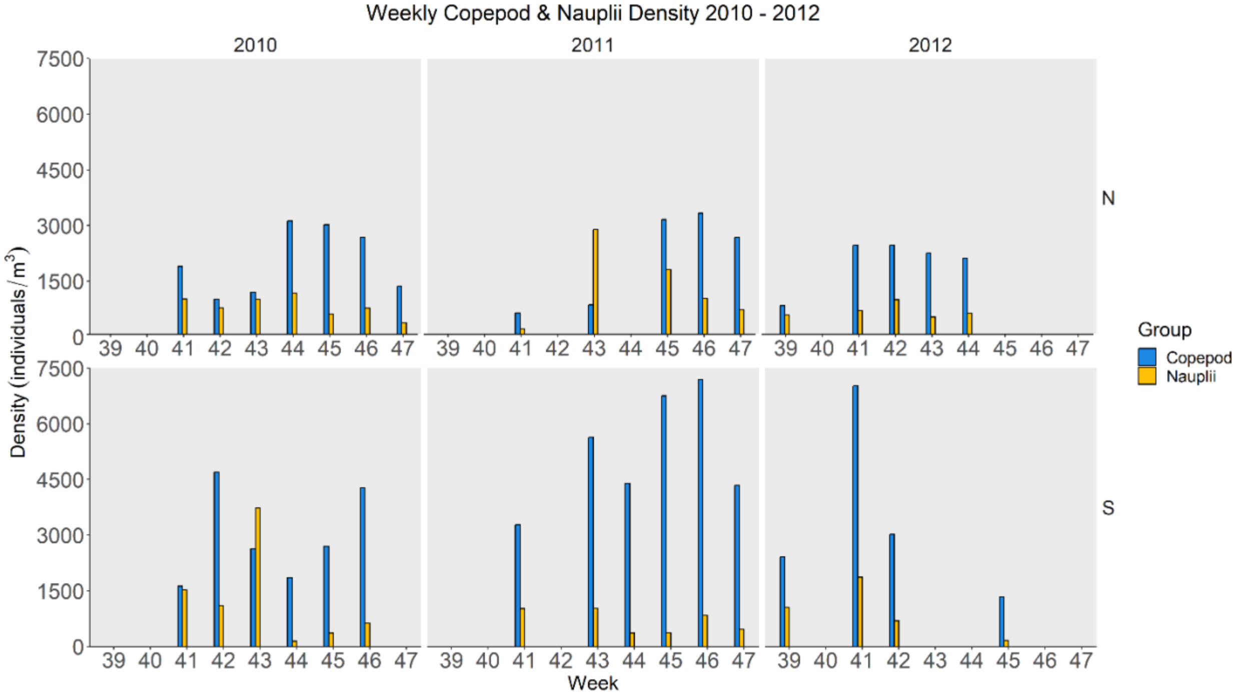

Figure 13: Weekly copepod & nauplii density at north and south stations for 2010 – 2011.

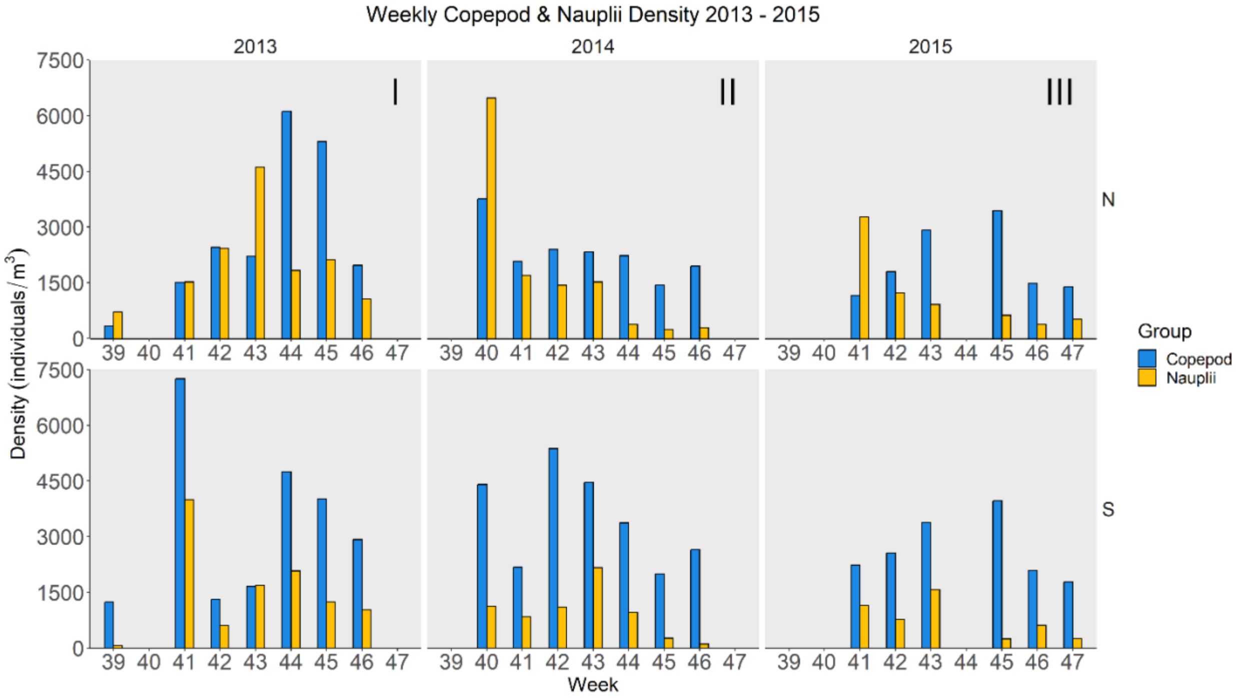

Figure 14: Weekly copepod & nauplii density at north and south stations for 2013 – 2015. “I” indicates mild MHW conditions in the Pacific Ocean, “II” indicates moderate MHW conditions in the Pacific Ocean, and “III” indicates severe MHW conditions in the Pacific Ocean.

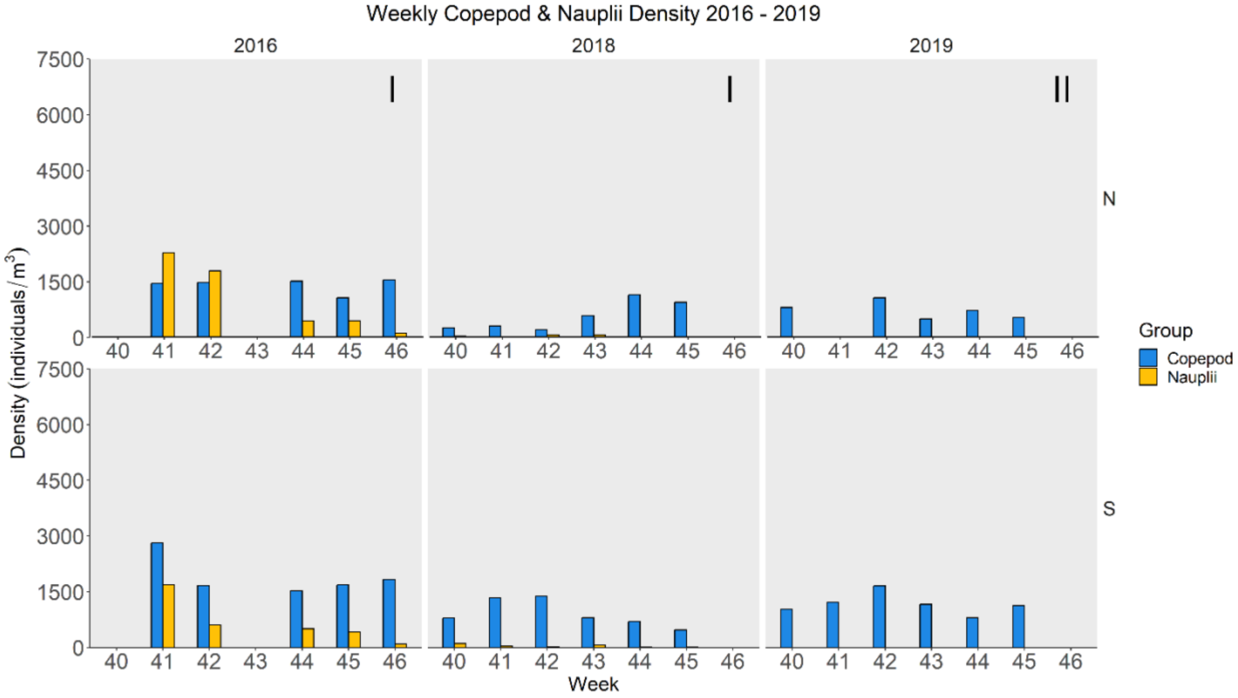

Figure 15: Weekly copepod & nauplii density at north and south stations for 2016 – 2019. “I” indicates mild MHW conditions in the Pacific Ocean and “II” indicates moderate MHW conditions in the Pacific Ocean. Note that copepod nauplii were not counted in 2019.

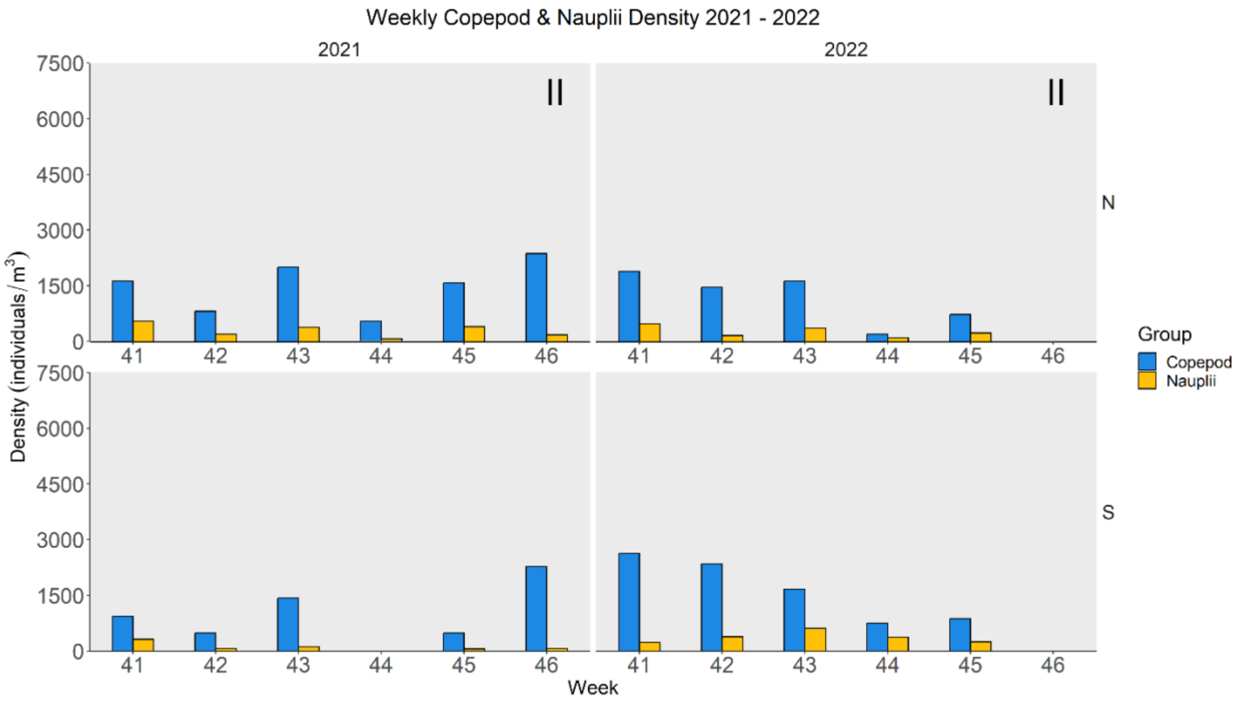

Figure 16: Weekly copepod & nauplii density at north and south stations for 2021 and 2022. “II” indicates moderate MHW conditions in the Pacific Ocean.

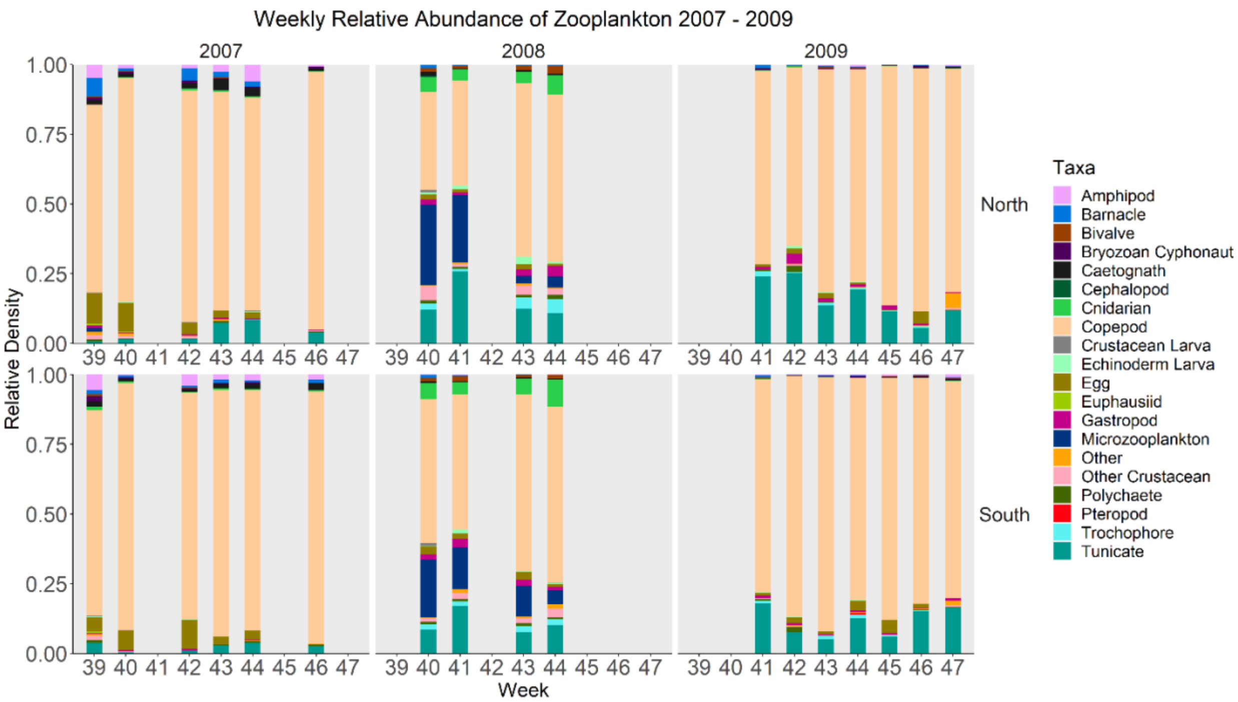

Figure 17: Weekly relative abundances of zooplankton at North and South stations from 2007 – 2009.

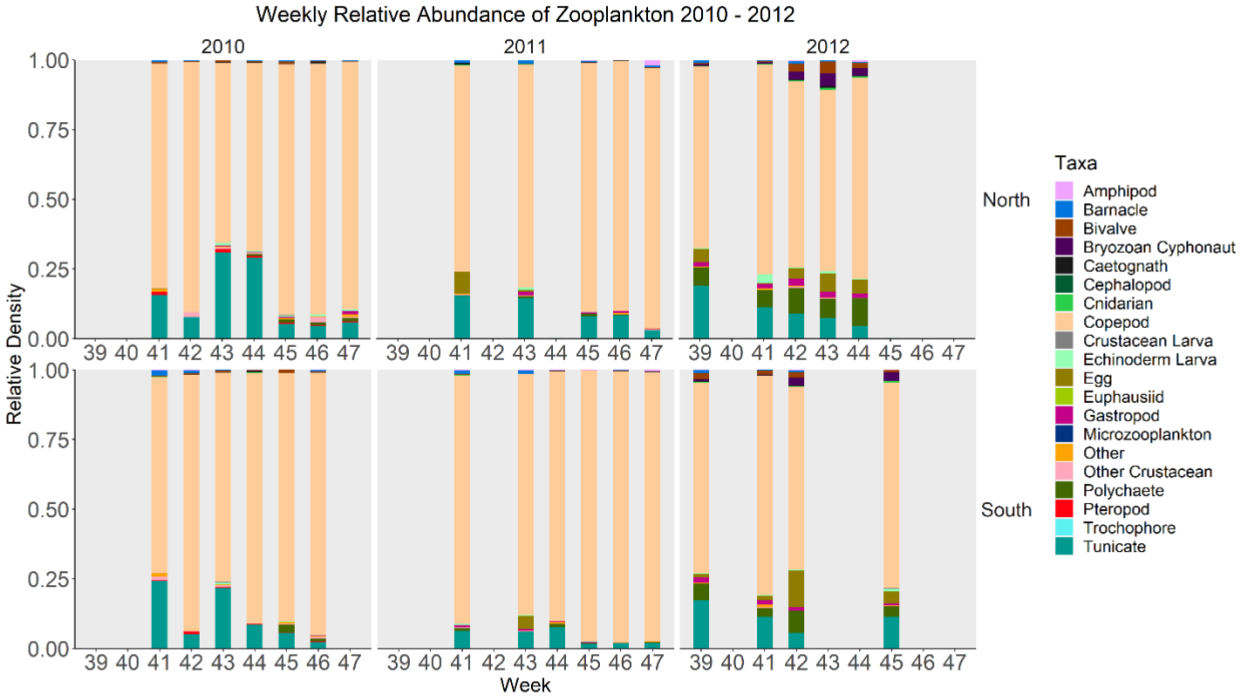

Figure 18: Weekly relative abundances of zooplankton at North and South stations from 2010 – 2012.

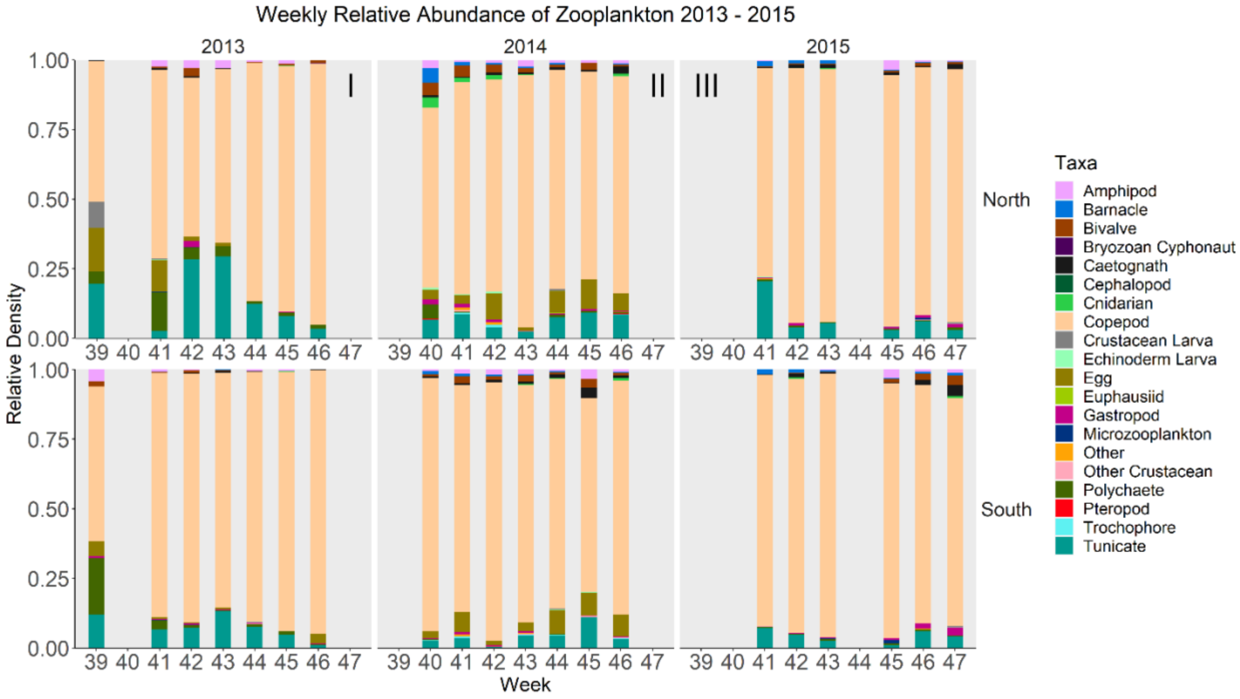

Figure 19: Weekly relative abundances of zooplankton at North and South stations from 2013 – 2015. “I” represents mild MHW conditions, “II” represents moderate MHW conditions, and “III” represents severe MHW conditions.

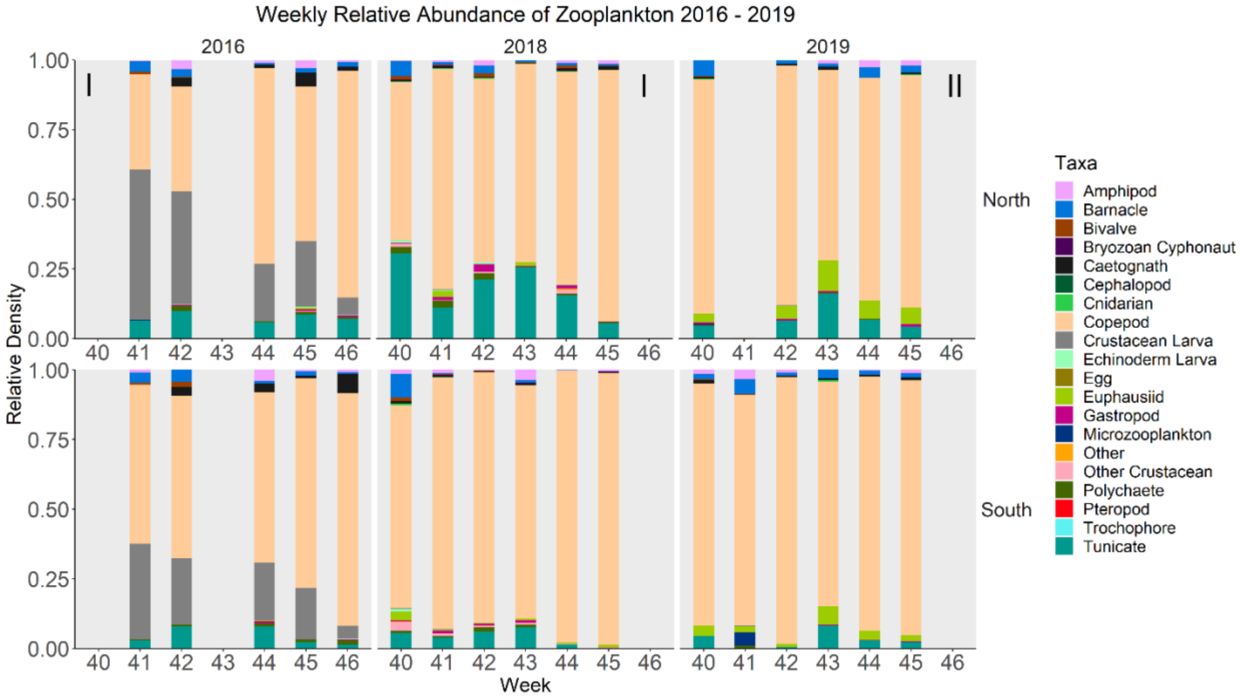

Figure 20: Weekly relative abundances of zooplankton at North and South stations from 2016 – 2019. “I” represents mild MHW conditions and “II” represents moderate MHW conditions.

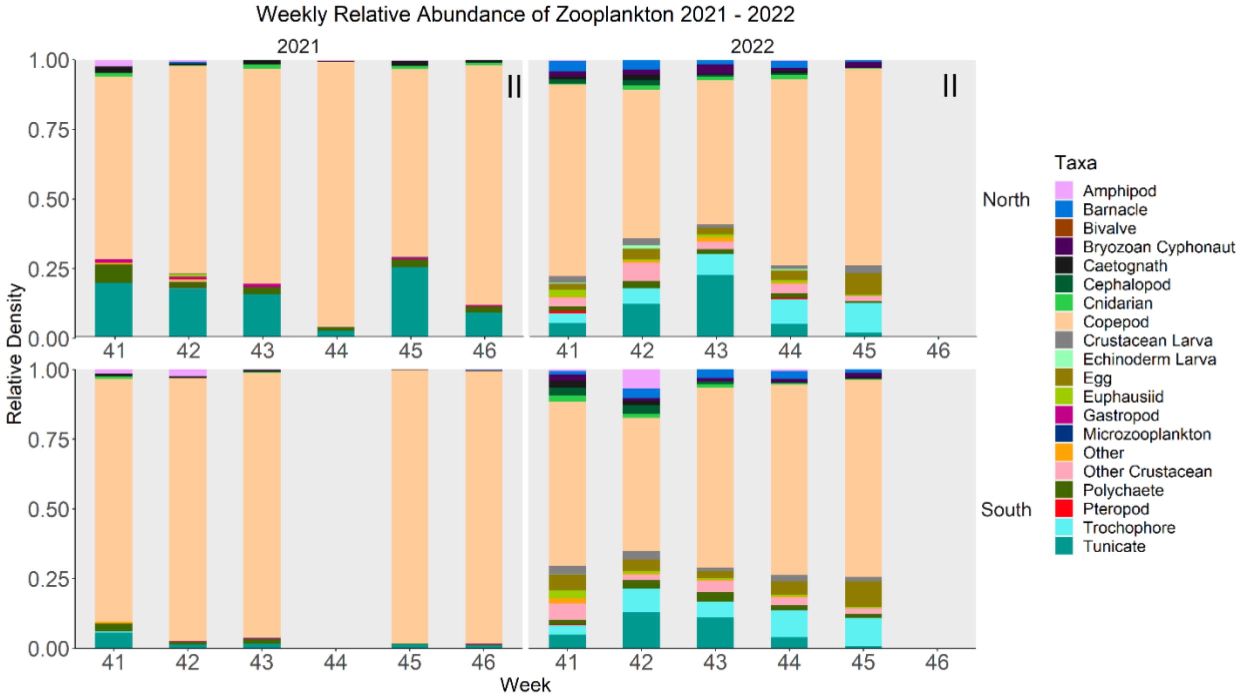

Figure 21: Weekly relative abundances of zooplankton at North and South stations in 2021 and 2022. “II” represents moderate MHW conditions.